J Mater Sci (2011) 46:3370–3377
DOI 10.1007/s10853-010-5225-6

Effect of carbon nanotube reinforcement on fracture strength of composite adhesive joints

Garrett L. Burkholder · Young W. Kwon · Randall D. Pollak

Received: 27 October 2010 / Accepted: 24 December 2010 / Published online: 7 January 2011

Abstract This study investigated the use of carbon nanotubes (CNTs) as an epoxy adhesive additive for adhesive joints between steel–composite interfaces and composite–composite interfaces. The study also examined the effect of CNT functionalization to improve CNT dispersion and thus improve joint strength. Specimens were constructed by adhesively bonding two parallel coupons, with a starting crack at one end. The specimens were loaded to final failure in three-point bending for Mode II fracture. Critical strain energy release rate was used to compare fracture properties of each set of specimens. It was shown that additions of multi-walled CNTs on the order of 1 wt% with diameters on the order of 30 nm and lengths 5–20 μm enhanced fracture toughness for both steel–composite and composite–composite adhesive joints tested. However, other combinations of CNTs could significantly decrease fracture properties, likely due to agglomeration issues. Functionalization of nanotubes showed some limited promise. Scanning electron microscopy validated the improved dispersion of CNTs using functionalization, but also highlighted the shortening effects due to the harsh chemical treatment. In summary, the study illustrates the importance of various CNT parameters on fracture properties, and encourages further investigation and optimization of these parameters for applications of interest.

G. L. Burkholder · Y. W. Kwon (✉) · R. D. Pollak
Department of Mechanical and Aerospace Engineering,
Naval Postgraduate School, 700 Dyer Road, Mail Stop: ME/Kw,
Monterey, CA 93943, USA
e-mail: ywkwon@nps.edu

Introduction

Large composite structures in place of traditionally metallic structures have been increasingly used in engineering design over the past two decades, in particular, the aerospace industry in which weight savings are of critical importance. More recently, the use of composites has received more attention in naval construction [1]. One of the major challenges in ship design is weight distribution, which is ever more difficult with the continuing trend of larger radars and communication suites which add significant weight above the water line, negatively impacting ship stability and handling. For such structures, composites generally offer increased strength and corrosion resistance at a reduced weight compared to their metal alternatives. Thus, the use of carbon fiber reinforced polymers (CFRPs) in the above-water superstructure has been envisioned for next-generation warships.

One of the challenges facing the introduction of composites as a superstructure material is the need for joining composite sections to other composite or metallic sections. This joining may be required during initial modular construction, repair of damaged articles, or replacement of older metallic components with new composite components. These joint interfaces generally involve discontinuity of the reinforcing fibers and higher stress concentrations. Of course, this challenge is by no means unique to naval construction, and has also frustrated other applications such as aircraft construction. During developmental testing, the F/A-18 Hornet, which pioneered the use of a composite-to-metal interface through the primary load path of the wing root, encountered matrix-dominated delamination near the adhesively bonded step lap joint which linked the graphite epoxy wing to the titanium root [2]. Bolts were eventually added to the adhesive joint to provide confidence in the

structural integrity. Similar issues plagued development of the Boeing 787 Dreamliner [3]. The wings are stiffened by composite stringers attached to the skin and titanium root, and flexural stresses in testing led to delamination problems requiring a late redesign of the stringers and addition of fastener bolts, causing production delays. More examples could follow, but it is enough to say that improving the structural integrity of such joints is both a challenge and a priority.

Recent study has addressed the testing and analysis of one particular type of joint used for composite-to-composite interfaces, namely, the scarf joint (bonded through polymer matrix curing) [4]. Follow-on work considered strength enhancement in compression of such a joint using dispersed carbon nanotubes (CNTs) along the interface [5]. CNTs may be categorized as single-, double-, or multi-walled based on the number of concentric graphene sheets rolled together to make up the nanotube, and have shown promise for improving mechanical, electrical, and thermal properties for many applications. Additional study has demonstrated that CNTs along a fully bonded scarf joint interface could improve Mode I and Mode II fracture toughness [6]. Moreover, the use of CNTs along such joints has shown promise for interfacial damage detection through changes in electrical resistance as the highly conductive CNT network was disrupted by crack growth [7]. For bonding of composites to metals, metal wire joints have also been recently studied, for which co-cured metal wire and fibrous composite showed promise for joining such dissimilar sections [8, 9].

The adhesive joint is an alternative to the composite scarf joint or the metal wire joint, and is attractive for a wide variety of joining applications, such as bonding of composite sections to other composite, steel, titanium, or aluminum components. Adhesives are particularly attractive due to their simplicity and ability to be applied in remote and austere environments, such as the deck of a ship undergoing repairs. As with the composite scarf joint, research has shown that dispersion of CNTs can improve strength characteristics of adhesively bonded joints [10]. However, a common problem encountered in applications requiring dispersed CNTs is ensuring their uniform dispersion. CNTs have a tendency to attract each other and become clustered. In order to overcome this tendency, mechanical means of dispersion such as high shear mixing and sonication have been studied for nanocomposites [11–13]. Surfactants are also used to aid in the dispersion of CNTs. More recently, chemical functionalization of the CNTs has drawn interest.

A functionalized CNT is one in which a chemical group (such as a carboxyl group or amine) is bonded to the surface of the nanotube. Once the initial functionalization has taken place, any number of different functional groups can replace or augment the initial group using established chemistry techniques. Careful selection of the functional group can significantly improve chemical bonding between the CNT and matrix or adhesive material. Chemical functionalization of CNTs has been shown to improve the mechanical and electrical properties of nanocomposites with a wide variety of matrix materials [14–18].

This study focused on the use of adhesive joints (between flat parallel faces) to bond steel–composite and composite–composite sections of interest for naval construction, although the results are applicable to other applications as well. The objectives were to investigate how the addition of various CNTs in the adhesive (thus forming a nanocomposite adhesive) affected fracture strength in Mode II loading, with particular interest in the use of functionalization to improve CNT dispersion and thus affect joint strength. The basic procedure was to prepare two coupons for each specimen, adhesively bond the coupons together with a starting crack, and then subject the specimen to a three-point bend test to produce Mode II loading over the crack, increasing the load until failure. Upon failure, the Mode II critical strain energy release rate would be determined and used as the mechanical property of merit for comparisons. Scanning electron microscopy (SEM) was used to validate functionalization of the CNTs.

Materials and methods

Materials selection and preparation

Materials were selected in communication with Naval Surface Warfare Center (NSWC) Carderock Division to represent structural materials used in naval construction. Selection rationale and preparation details are summarized in the following sections.

Steel

Steel test coupons were made from plain carbon steel, with 1018 steel chosen as it is cold rolled and requires little surface preparation prior to adhesion compared to hot-rolled alternatives. The steel came as 3.175-mm thick bar stock. Steel surfaces were initially cleaned with reagent-grade acetone to remove grease and organic build up. The surface was then roughed up using glass beads in a sand blaster, and residual beads were removed with dry compressed air. Finally, the surface was wiped with a lint-free rag to remove any remaining debris. All surfaces were bonded within several hours to one week of the glass bead abrasion to ensure a consistent clean surface. No differences were observed between coupons which were abraded

the same day as bonding and those abraded several days before bonding.

Carbon fiber composite

CFRP coupons were constructed of TORAY T700CF carbon fiber weave with a DERAKANE 510-A40 vinyl-ester matrix. The DERAKANE 510-A40 had to be cured and hardened. The ratios of the hardening chemicals, methyl ethyl ketone peroxide (MEKP), and 6% cobalt naphthenate (CoNap), as well as an accelerator, dimethylaniline (DMA), can be varied to control gel time of the resin based on ambient temperature. To ensure complete wetting of the carbon fibers, the desired gel time was between 45 to 60 min. At the ambient temperature of 21 °C, the addition of 1.25% MEKP (by weight), 0.2% CoNap, and 0.03% DMA resulted in an acceptable gel time.

CFRP coupons were fabricated using Vacuum-Assisted Resin Transfer Molding (VARTM), as described in previous studies [5–7]. Individual panels were fabricated to approximately 410 mm by 360 mm to provide fifteen 25 mm by 305 mm test coupons. This was about the largest panel that could be created using VARTM in the laboratory. For testing of dissimilar materials, the bending stiffness of each material must be matched across the bond line to ensure the bonding surface acts as the neutral axis in bending. As the steel came in a standard thickness, the thickness of the CFRP coupons was adjusted to match the bending stiffness of the steel. In order to create a composite with the same stiffness as 3.175-mm thick 1018 steel, 13 layers of carbon fiber fabric were required for each sample based on Young's modulus of 205 and 52.4 GPa for the steel and carbon fiber composite, respectively.

Coupons were cut from panels with a water jet and allowed to cure at least 7 days prior to bonding. Surfaces were lightly sanded with 80-grit sandpaper to expose some fiber and create a slightly roughed-up surface for bonding. Following abrasion, the surface was wiped with reagent-grade acetone to remove any organic compounds, allowed to dry, and wiped with a lint-free cloth to remove any remaining debris. The surfaces were then bonded within a day.

Carbon nanotubes

A variety of CNTs were considered, but multi-walled CNTs (MWCNTs) were selected based on previous research showing their capability to strengthen scarf joints of similar composite materials [5, 6]. The baseline MWCNTs had diameter 30 ± 15 nm and length 5–20 μm, designated PD30L520 by the vendor (NanoLab). In addition, nanotubes of shorter length (PD30L15), smaller diameter (PD15L520), and smaller diameter with bamboo structure (BPD15L520) were used. Bamboo-type nanotubes have internal transverse layers of carbon atoms which resemble the bulkheads within bamboo reeds.

Baseline nanotubes were also functionalized with an attached carboxyl group (written as PD30L520 w/COOH on graphs) to investigate the effects of functionalization. Believing that the adhesive had an amine-based hardener, a carboxyl group was recommended to functionalize the nanotubes for better dispersion [17].

CNT functionalization was accomplished using chemistry techniques at the United States Naval Academy (C. Whitaker C, 2009, United States Naval Academy, Personal communications). The MWCNTs (510 mg) were sonicated up to 10 h in 100 mL of mixed concentrated sulfuric/nitric acids (3:1). The mixture was then diluted with 800-mL distilled water and filtered. The solid was dried at room temperature and sonicated in a solution of 100-mL sulfuric acid and hydrogen peroxide (4:1) for 10 min. The reaction mixture was allowed to stand at room temperature for 1 h. After dilution with 800-mL deionized water, the mixture was filtered through a 0.2-μm Teflon® filter, washed with deionized water, and then dried overnight at 80 °C in a vacuum oven. This process terminated the open ends and sidewall defect sites of the MWCNTs with carboxylic acid groups (yielding 460 mg). Verification of CNT functionalization was accomplished using infrared (IR) spectroscopy, in which the IR absorption profile (in terms of wavelength) is used to characterize the composition of a sample, as bonds within different substances absorb IR energy at different wavelengths. Functionalized CNTs were imaged under SEM upon receipt, as described in "Scanning electron microscopy".

Adhesive

Two epoxy adhesives were considered for study based on current use in marine vessels: West Systems' G/flex and PRO-SET Epoxy. Selection was based on higher Mode II critical strain energy release rate (G_{IIc}) during preliminary testing (in accordance with "Mode II test method") of steel–composite and steel–steel specimens. Based on this preliminary testing, the G/flex adhesive was used for the study. This adhesive is a two-part epoxy (resin and hardener) engineered to maintain good strength characteristics while remaining flexible. Based on color and odor, the hardener was determined to be amine based.

Adhesion procedure

All adhesive was mixed in small batches by weight ratio, 1.2:1, resin to hardener. Typical batch size was 11–15 g. In a plastic cup, the adhesive mixture was stirred by hand to a consistent color and smooth texture, taking about

3 min. For tests in which nanotubes were added to the adhesive, CNTs were added after the resin, but prior to the hardener. Again the mixture was stirred by hand for 3 min until smooth and consistently colored.

Adhesive was applied to one of the two coupons making up a bonded test specimen using a plastic knife for an even surface layer. For steel–composite specimens, the adhesive was applied to the steel coupon. After adhesive application, a piece of Teflon® film was folded on itself to create an initial crack tip (described in next section). Generally, the crack tip was located 75–90 mm from the end of the specimen (of total length 305 mm). This location allowed a crack length of 50 mm with overall span length of 220 mm under three-point loading. The specimens were then clamped using evenly spaced spring clamps to ensure consistent pressure across the bond surface. The clamps were left on overnight while the glue cured. According to the manufacturer's data, 90% of full strength should be attained after 24 h of cure time. All samples were allowed to cure a minimum of 48 h prior to testing.

Mode II test method

In order to compare Mode II fracture toughness of each specimen, a basic three-point bending test was used to generate Mode II loading of the initial crack, as illustrated in Fig. 1. Testing was conducted on an Instron tension/compression machine (model number 4507/4500) with a 10-kN load cell. A constant deflection rate of 1 mm/min was used for all tests. A typical load–displacement curve is shown in Fig. 2. Under the displacement-controlled loading, crack repeatedly grew and stopped until it propagated to the center of the specimen where the loading was applied.

The Mode II critical strain energy release rate, G_{IIc}, was used as a measure of the fracture toughness, and was calculated using the compliance method as described below [6]:

$$G_{II} = \frac{9a^2P_c^2C}{2b(2L^3 + 3a^3)} \quad (1)$$

where G_{II} is the critical energy release rate, a is the initial crack length, b is the coupon width, L is the half span length, P_c is the critical load determined based on the local maximum or slope change in the load–displacement curve as shown in Fig. 2, and C is the compliance of the curve. For steel–composite specimens, the composite side was always on the opposite side of the load cell.

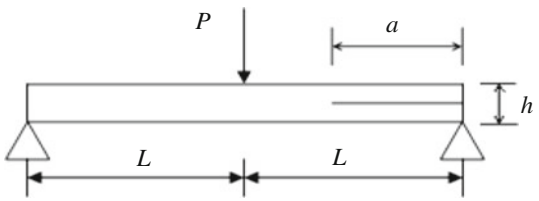

Fig. 1 Test geometry (load P, initial crack length a, thickness h, half-span length L)

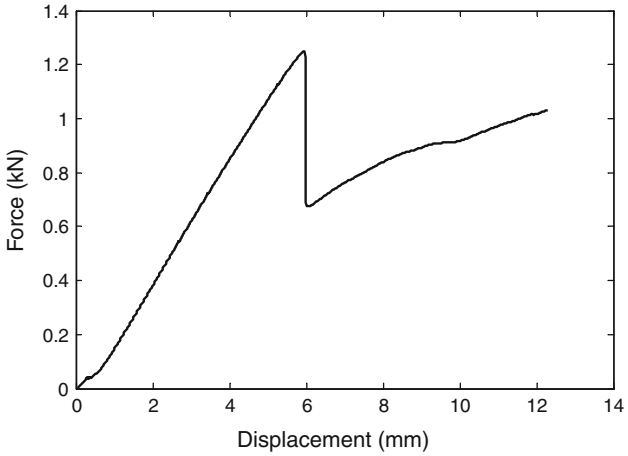

Fig. 2 Load–displacement curve for composite–composite specimen undergoing Mode II testing

Scanning electron microscopy

SEM was used to compare carboxyl-functionalized MWCNTs to similar MWCNTs without functionalization. Analysis was accomplished using a Carl Zeiss Neon 40 SmartSEM V05.03 Field Emission Scanning Electron Microscope at beam energies of 2 and 20 keV. Preparation included dispersion of MWCNTs in ethanol, water bath sonication for 10 min, and then placement on a copper grid. Once on the copper grid, the ethanol evaporated and the residual CNT network could be analyzed in the SEM, with results described in the next section.

Functionalization effects

Functionalization produced three observable changes to the MWCNTs: nanotube shortening, a wavier or rougher surface, and better dispersion. The first significant observation was that the functionalized nanotubes were considerably shorter than their pristine counterparts, a not unexpected result. Vendor specifications for the PD30L520 MWCNTs indicated a length of 5–20 μm. These lengths were validated by representative CNTs observed under SEM. However, functionalized CNTs had lengths on the order of 1–5 μm, illustrating the reduced aspect ratio (length/diameter) due to the harsh chemical treatment. In addition to shortening, surfaces of the functionalized nanotubes were rough under SEM, whereas the surfaces of the pristine

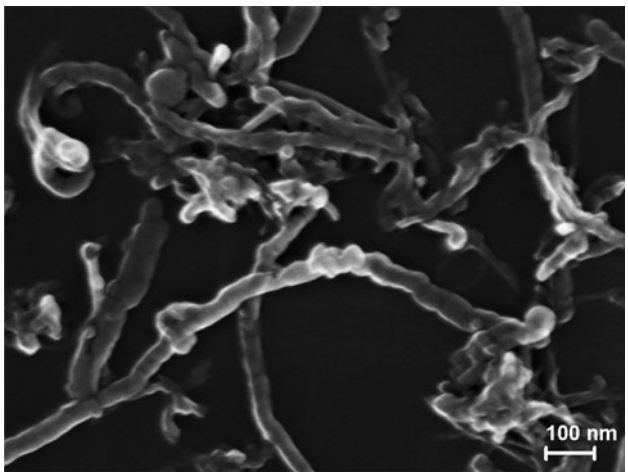

Fig. 3 Functionalized MWCNTs with rough surfaces

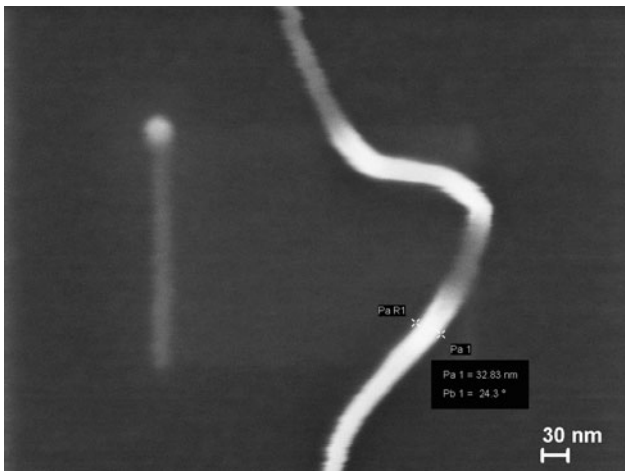

Fig. 4 Pristine MWCNTs with smooth surfaces

nanotubes were generally straight and sharp (Figs. 3, 4). The wavy appearance of the functionalized nanotubes is caused by the carboxyl group causing additional scattering of the electron beam. This rough appearance confirmed the presence of attached side groups. Lastly, the improved dispersion of functionalized nanotubes was validated under SEM.

Test results and discussion

Initial Tests Without CNTs

Both steel–composite and composite–composite joints without CNTs were tested as described in "Mode II test method" to ensure failures occurred through crack propagation across the bonding layer. Five steel–composite specimens were tested, with an average G_{IIc} value of 14,200 N/m when reported to three significant figures, with a 90% confidence interval of ±400 N/m using a two-tailed t statistic for the mean. Seven composite–composite specimens yielded an average G_{IIc} value of 10,300 (±800) N/m. The load–displacement curve for a composite–composite specimen is shown in Fig. 2. The general shape of the curve was the same for steel–composite specimens as well as any specimen including CNTs. The difference was for the slope of the curve and the peak force value depending on the specimen tested.

It was determined that bonding failure occurred through the adhesive itself, and thus should not have been very dependent on the materials being adhered so long as the failure occurred in the adhesive layer. To validate this assumption, both steel–steel and aluminum–aluminum joints were also tested (seven specimens each), where the aluminum was 5052 aluminum alloy common in marine construction. The steel–steel specimens yielded an average G_{IIc} value of 10,700 (±600) N/m, while the aluminum–aluminum specimens had an average of 11,000 (±2000) N/m. Failures again occurred within the adhesive layer. Thus, all adhesive joints between like materials had quite similar fracture toughness, regardless of the material (steel, aluminum, or composite). But the steel–composite joints had considerably higher fracture toughness as measured by G_{IIc}.

The higher Mode II critical strain energy release rate of the steel–composite bond was determined to be a result of the initial crack being located off the neutral axis in bending. Thus, the energy release rate represented was actually under mixed mode, not purely Mode II. The bond was located off the neutral axis because only a discrete number of carbon fiber layers could be used to create a composite sample, and thus only discrete values of composite thickness were available. Calculations indicated that 12.5 layers of carbon fiber should be used to produce a sample with the same bending stiffness as the 3.175-mm thick steel. Since 13 layers of carbon fiber were used to construct the sample, the bending stiffness did not exactly match and thus there was some mixed mode behavior for the steel–composite joints.

Steel–composite adhesive joints with CNT reinforcement

Various nanotube additions were studied to determine their effect on the strength of the steel–composite adhesive joint under Mode II loading (Fig. 5), with seven specimens tested for each nanotube configuration. The data in Fig. 5 have been normalized using the G_{IIc} value for the steel–composite adhesive joint without CNT reinforcement (14,200 N/m).

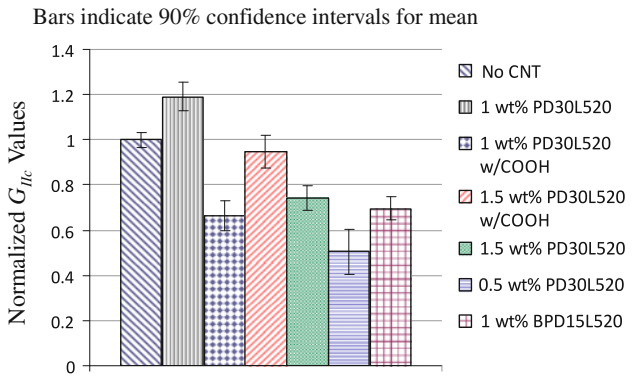

Fig. 5 Data for steel–composite adhesive joints

Effect of nanotube reinforcement

The addition of 1 wt% PD30L520 MWCNTs increased Mode II critical strain energy release rate by about 20% on average (this improvement was statistically significant at the 90% confidence level). It was also observed that the failure path shifted from through the adhesive to the interface between the adhesive and the bonded material when MWCNTs were added, suggesting that the adhesive layer was no longer the weakest link. Furthermore, for the samples with larger G_{IIc} values, more of the failure occurred through the steel–adhesive interface (Fig. 6), while samples with lower G_{IIc} values exhibited more failure through the composite–adhesive interface (Fig. 7).

These results show that when MWCNTs are dispersed in the adhesive layer, the strength of the adhesive layer may be enhanced to the point that failure through the adhesive layer is no longer the primary failure mechanism under load. Thus, dispersion of nanotubes within the adhesive has been shown to increase the strength of steel–composite

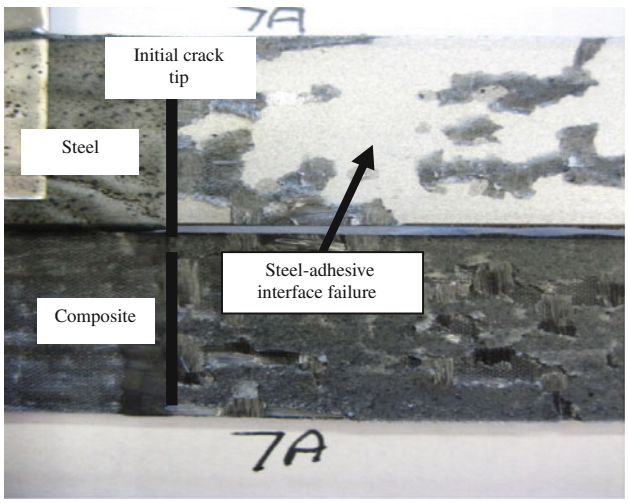

Fig. 6 Failure along composite interface in steel–composite joint

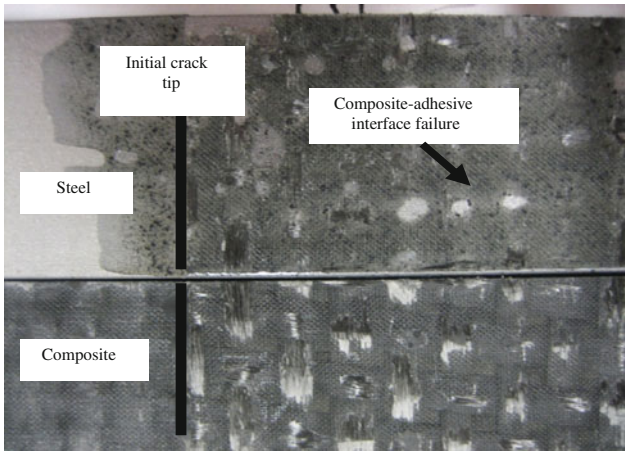

Fig. 7 Failure along composite interface in steel–composite joint

joints. But not all combinations of nanotubes will produce equal results; some additions can decrease the joint strength. Controlling the agglomeration of nanotubes can be a significant factor in determining whether their addition improves mechanical properties.

Effect of nanotube functionalization

As functionalization can improve dispersion, one might expect the use of functionalized MWCNTs within the adhesive to improve the joint strength under Mode II loading. However, Fig. 5 shows the addition of 1 wt% carboxyl-functionalized MWCNTs resulted in an average G_{IIc} value just 65% of that without nanotube reinforcement. Increasing the concentration to 1.5 wt% resulted in a statistically insignificant G_{IIc} difference compared to the joint without nanotubes. It is important to note, however, that use of functionalized nanotubes at the 1.5 wt% level yielded better results than pristine nanotubes at comparable concentration. Thus, functionalization indeed showed promise, however this study did not set out to optimize the parameters (such as concentration and length) for best results. Shortening of the nanotubes during the functionalization process surely had a negative impact on strength of the adhesive, thus countering any gains due to better dispersion.

Effect of nanotube concentration

When the concentration of MWCNTs was increased to 1.5 wt%, the average G_{IIc} value fell to about 70% of the bond without nanotubes (Fig. 5). Decreasing the weight percent of MWCNTs to 0.5% also reduced the average G_{IIc} value to 50% of the original strength. The failure occurred through the composite–adhesive interface, and the amount of carbon fiber that was torn out was also reduced when the

concentration of MWCNTs was either increased or decreased. These results show that for a given type of nanotube, there is some optimum concentration to improve joint strength. Above or below this optimal concentration, the joint strength may actually be diminished.

Effect of bamboo structure

The final parameter to be studied was the use a bamboo-structured nanotube. The addition of 1 wt% BPD15L520, a bamboo structure nanotube with diameter 15 nm and length 5–20 μm, resulted in a bond with 70% of the average G_{IIc} of the original bond (Fig. 5). Again, the failure surface was generally through the composite–adhesive interface and there was little carbon fiber tear out noted on the failure surface. As the bamboo nanotubes also had a smaller diameter (nominally 15 vs. 30 nm), the individual effects of nanotube structure and diameter cannot be discriminated. It is hypothesized that bamboo nanotubes may improve results because, like bamboo itself, their structures provide greater stiffness, perhaps making them more resilient to curling and agglomeration, and thus easier to disperse. Initial results, however, were inconclusive.

Composite–composite adhesive joints with CNT reinforcement

The final group of tests evaluated adhesive joints between two carbon fiber composite coupons. This test group looked at the effects of functionalization, concentration, nanotube length, and nanotube diameter. Results are summarized in Fig. 8. As was the case for steel–composite tests, each nanotube configuration was tested using seven specimens.

The addition of 1 wt% pristine MWCNTs resulted in a 30% increase in average G_{IIc}. This increase was statistically significant using 90% confidence intervals. Thus, the addition of MWCNTs to the adhesive was shown to significantly improve the strength under Mode II loading, as was the case with steel–composite joints.

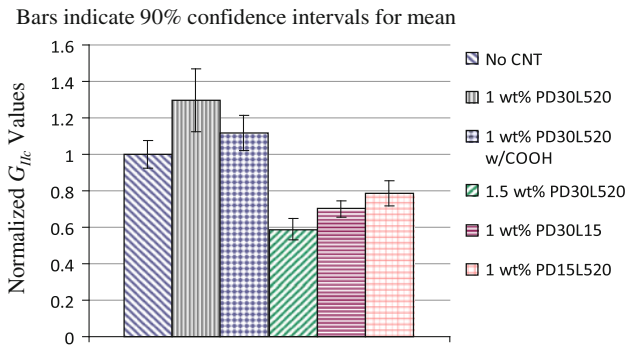

Fig. 8 Data for composite–composite adhesive joints

The addition of 1 wt% carboxyl-functionalized MWCNTs improved the average G_{IIc} value by only about 10%. Again, the nanotube shortening due to the harsh chemical treatment during functionalization is likely responsible for the decreased strength compared to pristine CNTs. Tests at 1.5 wt% of functionalized MWCNTs were not accomplished during this phase. As with the steel–composite joint, increasing the pristine MWCNT concentration to 1.5 wt% resulted in a much weaker bond. Addition of MWCNTs beyond 1 wt% appears to impact bonding in a negative manner, due to agglomeration and/or reduced bonding between the resin and adhesive.

For the composite–composite joint, tests were also accomplished with shorter length pristine nanotubes. The addition of 1 wt% PD30L15, a nanotube with a length of only 1–5 μm, resulted in an average G_{IIc} value only 70% that of the non-reinforced joint. Considering that the functionalization process reduced nanotube length from 5–20 μm to about 1–5 μm, these PD30L15 results can be compared to those with functionalized PD30L520 to isolate the effect of functionalization. Both sets of specimens thus had the same multi-wall structure, same concentration, same nanotube diameter, and same effective length, but the functionalized specimens yielded significantly higher G_{IIc} values. This comparison illustrates the promise of functionalization, showing that positive results may have been masked by the shortening effect.

Finally, the addition of 1 wt% PD15L520, a nanotube with a diameter of 15 nm resulted in the G_{IIc} values that were on average only 80% of the unreinforced value. This result indicates that decreasing nanotube diameter may reduce strength, all else equal. Thus, the smaller diameter bamboo nanotubes tested for the steel–composite joint ("Effect of bamboo structure") may indeed have had lower strength due to the smaller diameter, rather than due to the bamboo structure.

From the present and past studies [5, 6], it was suggested that the CNTs provides resistance to crack growth through micromechanical interlocking of clustered CNTs. As a result, in general, the longer was the CNT, the more effective was the CNT for increasing fracture strength. An optimal concentration of CNTs was also necessary to increase the fracture strength. Too low concentration of CNT did not provide enough micromechanical interlocking of CNT while too high concentration of CNT resulted is sliding among CNTs with just van der Waals force.

Conclusions

It was shown for both steel–composite and composite–composite adhesive joints that the dispersion of MWCNTs in the adhesive can improve fracture properties. As recent

research has exploited the electrical conductivity of CNT networks to monitor crack growth along composite interfaces (while also strengthening these interfaces), adhesive joint strengthening using CNTs may also allow simultaneous damage monitoring. It was shown that nanotube functionalization, concentration, structure, length, and diameter all played a significant role in determining whether nanotube addition strengthened or weakened the adhesive joint.

Functionalization of the MWCNTs resulted in better dispersion of the nanotube network, while also shortening the nanotubes. When added to the adhesive, functionalized MWCNTs produced better results than pristine MWCNTs of similar length for the composite–composite joint. Further research is required to optimize the parameters (e.g., concentration, length, side groups, and diameter) for specific bonding cases. Ideally, the specific characteristics of the adhesive of interest would be better known and the functional group could be tailored to chemically react and harden into the adhesive matrix.

Depending on the CNT parameters, adhesive, and loading mode; there exists some optimum concentration of CNTs to produce the best strengthening effect. In general, this optimum was in the neighborhood of 1 wt% for tests conducted as part of this project. Testing also showed that shorter length nanotubes resulted in weaker bonding in the composite–composite joint tests. Smaller nanotube diameter also produced weaker bonding in the composite–composite tests, all else equal. The key takeaway is that the addition of CNTs is not as straightforward as one might hope in improving fracture characteristics, but rather presents an optimization challenge to get the right length, diameter, concentration, and degree of functionalization to maximize the joint strength.

Acknowledgements The authors gratefully acknowledge the Naval Surface Warfare Center's Carderock Division for both financial and technical support; the Office of Naval Research's Solid Mechanics Program for funding support; Professor Craig Whitaker of the United States Naval Academy's Chemistry Department for preparation and IR spectroscopy of functionalized nanotubes; Professor Sarath Menon of the Naval Postgraduate School for assistance with SEM imaging; and Dr. Chanman Park of the Naval Postgraduate School for mechanical test support.

References

1. Mouritz AP, Gellert E, Burchill P, Challis K (2001) Compos Struct 53:21
2. Jones R, Alesi H (2000) Compos Struct 50:417
3. Gates D (2009) Boeing 787 May Not Fly this Year. The Seattle Times, 22 July 2009
4. Kwon YW, Marron A (2009) Appl Compos Mater 16:365
5. Kwon YW, Slaff R, Bartlett S, Green T (2008) J Mater Sci 43:6695. doi:10.1007/s10853-008-2689-8
6. Faulkner SD, Kwon YW, Bartlett S, Rasmussen EA (2009) J Mater Sci 44:2858. doi:10.1007/s10853-009-3378-y
7. Bily MA, Kwon YW, Pollak RD (2010) Appl Compos Mater 17:347
8. Kwon YW, Schultz W, Loup DC, Rasmussen EA. ASME J Press Vessel Technol (accepted)
9. Klopfer J (2009) An experimental study of fiberglass composites containing metal-wire joints. Master's thesis, Naval Postgraduate School
10. Sun Y, Meguid SA, Liew KM, Ong LS (2004) Nanotechnology 3:126
11. Gojny FH, Wichmann MHG, Köpke U, Fiedler B, Schulte K (2004) Compos Sci Technol 64:2363
12. Andrews PM, Jacques D, Minot M, Rantell T (2002) Macro Mater Eng 287:395
13. Qian D, Dickey EC, Andrews R, Rantell T (2000) Appl Phys Lett 76:2868
14. Breton Y, Desarmot G, Salvetat JP, Delpeux S, Sinturel C, Berguin F, Bonnamy S (2004) Carbon 42:1027
15. Shen J, Huang W, Wu L, Hu Y, Ye M (2007) Compos Sci Technol 67:3041
16. Liu L, Wagner HD (2005) Compos Sci Technol 65:1861
17. Zou W, Du Z, Liu Y, Yang X, Li H, Zhang C (2008) Compos Sci Technol 68:3259
18. Kim JY, Han SI, Hong S (2008) Polymer 49:3335